

# INTERNATIONAL SOCIETY FOR SOIL MECHANICS AND GEOTECHNICAL ENGINEERING



*This paper was downloaded from the Online Library of the International Society for Soil Mechanics and Geotechnical Engineering (ISSMGE). The library is available here:*

<https://www.issmge.org/publications/online-library>

*This is an open-access database that archives thousands of papers published under the Auspices of the ISSMGE and maintained by the Innovation and Development Committee of ISSMGE.*

# A three-dimensional elasto-plastic model for sands

## Le modèle élastique et plastique du sable à trois dimensions

PU, JIA-LIU, Lecturer, Dept. of Hydraulic Engg., Tsinghua University, Beijing, China  
 LI, GUANG-XIN, Lecturer, Dept. of Hydraulic Engg., Tsinghua University, Beijing, China  
 SUN, YUE-SONG, Lecturer, Dept. of Hydraulic Engg., Tsinghua University, Beijing, China

**SYNOPSIS** Experimental and theoretical studies on 3-D yield function have been made. The suggested 3-D yield function is verified by making a comparison between calculated and experimental stress-strain relationship of medium dense Chengde sand under plane strain condition.

### INTRODUCTION

To determine the plastic potential function directly from test data by selecting appropriate workhardening rule so as to make the yield surface coincide with the plastic potential surface, i.e.  $f=g$ , has been proved feasible (Huang, 1980 1981). On this basis, different kinds of tests, including plane strain and true triaxial tests, have been made on sand under monotonic loading and repeatedly loading-unloading conditions. A 3-D (three dimensional) elastoplastic model is proposed with yield function and plastic potential function derived from test results. Method of determining the relevant parameters from conventional triaxial test is given. Stress-strain relationship of medium dense Chengde sand under plane strain condition derived by using this model is compared with the results obtained from plane strain tests.

besides the monotonic loading tests. Fig. 1 shows some typical stress-strain curves thus obtained. The volumetric strain during unloading seems to be always contractive irrespective of density and ambient pressure  $\sigma_3$ .

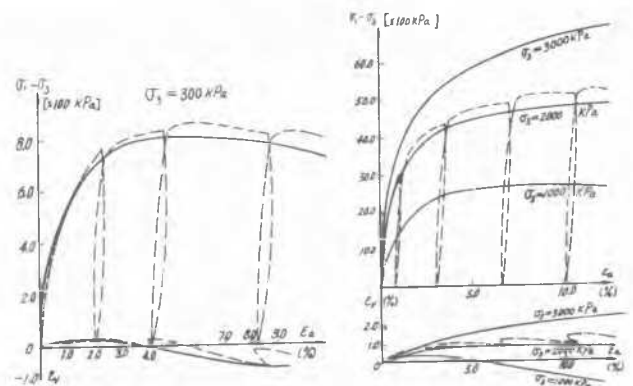


Fig.1 Typical stress-strain curves for sand obtained from triaxial compression tests

### EXPERIMENTS

The Chengde sand used has the following characteristics:

Median diameter	$d_{50}=0.18 \text{ mm}$
Uniformity coefficient	$d_{60}/d_{10}=2.8$
Specific gravity	$G_s = 2.63$
Maximum void ratio	$e_{max} = 0.80$
Minimum void ratio	$e_{min} = 0.40$

Test specimens were prepared by method of pluviating through water with simultaneous vibration. This method has been proved to yield good uniformity and high degree of saturation. Correction has been made for the effect of membrane penetration on volumetric strain.

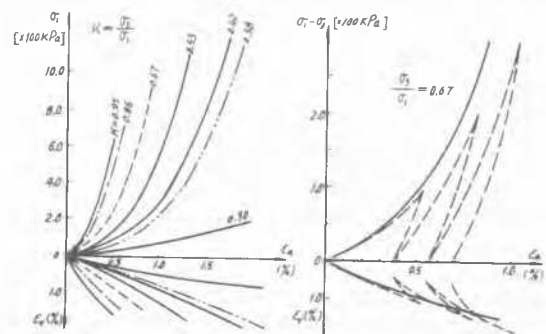


Fig.2 Stress-strain relation for sand obtained from  $\sigma_3/\sigma_1 = \text{constant}$  tests

### Conventional Triaxial Tests

Conventional drained triaxial compression tests were made with various densities ( $D_r=41\%, 64\%, 95\%$ ) and confining pressures ( $\sigma_3=100, 300, 500, 1000, 2000, 3000 \text{ kpa}$ ). In order to separate the elastic strain from the total strain, repeatedly loading-unloading tests have been carried out

Triaxial tests with the following stress paths have also been conducted:

1. Octahedral normal stress  $p=(\sigma_1+2\sigma_3)/3 = \text{const}$
2. Ratio of minor to major principal stress

$$K = \sigma_3/\sigma_1 = \text{const}$$

3.  $K_0$  consolidation

The stress-strain curves for  $K = \sigma_3/\sigma_1 = \text{const}$  tests are shown in Fig.2. It can be seen that the relation between deviatoric stress  $(\sigma_1 - \sigma_3)$  and axial strain  $\epsilon_a$  is of exponential type, curves corresponding to unloading and reloading stages do not form hysteresis but are of serrated shape, whereas the relation between axial strain  $\epsilon_a$  and volumetric strain  $\epsilon_v$  is approximately linear.

Plane Strain Tests

Tests were carried out under isotropic consolidation condition. Specimens of rectangular cross section 42mmx51mm with height 90mm were used. Dry densities were controlled within the limit of  $1.67 \pm 0.1 \text{ kN/m}^3$ . Test results for monotonic loading and repeatedly loading-unloading are shown in Fig. 3,4,5. It can be seen from Fig.3 that the initial tangent modulus of stress-strain curves and the peak deviatoric stress in plane strain tests are higher than those obtained from conventional triaxial tests. Angle of shearing resistance is about  $5^\circ$  higher, but the ultimate strength is nearly the same. The axial strain reached at peak deviatoric stress in plane strain condition is much smaller than that observed in

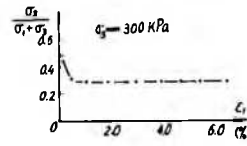


Fig.5  $\sigma_2/(\sigma_1 + \sigma_3) - \epsilon_1$  curve for sand in plane strain test

conventional triaxial tests. Fig.5 indicates that the value of  $\sigma_2/(\sigma_1 + \sigma_3)$  dropped rapidly from 0.5 corresponding to isotropic consolidation to 0.3 and maintained at this value up to failure. It may be noted from Fig.4 that there were residual stresses measured when  $(\sigma_1 - \sigma_3)$  were completely unloaded. The value of residual stress increased with number of repeating cycles. This may be an indication of the nature of soil as an elasto-plastic material.

True Triaxial Tests

True triaxial tests were carried out with constant  $\sigma_3$  and constant  $b = \sigma_2 - \sigma_3 / \sigma_1 - \sigma_3$  by varying proportionally the major and intermediate principal stresses  $\sigma_1$  and  $\sigma_2$ . Values of  $b$  used were 0, 0.25, 0.50, 0.75 and 1.00 with  $\sigma_3 = 100, 300$  and  $500 \text{ kpa}$  respectively. Typical stress-strain curves obtained for the case of  $\sigma_3 = 300 \text{ kpa}$  are as shown in Fig.6 from which it can be seen that an increase in parameter  $b$  will result in a steeper curve, higher peak strength and smaller strain at peak deviatoric stress. But as  $b$  increases, there will be greater volumetric contraction, less dilatation and steeper hysteresis loop for loading-unloading-reloading. The shape of volumetric strain versus axial strain curve is no longer serrated but looped. The above test results clearly demonstrate that the stress-strain relation of soil is very complicated. It is significantly affected by the stress path, stress history, stress level as well as the manner by which the load is applied.

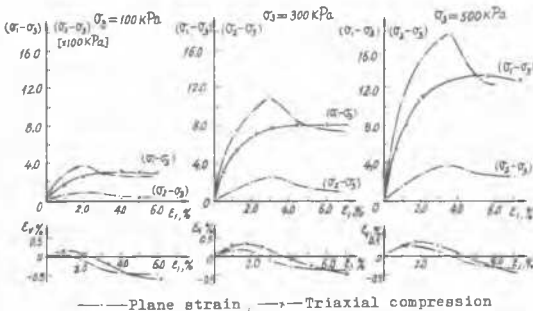


Fig.3 Triaxial and plane strain test curves for sand

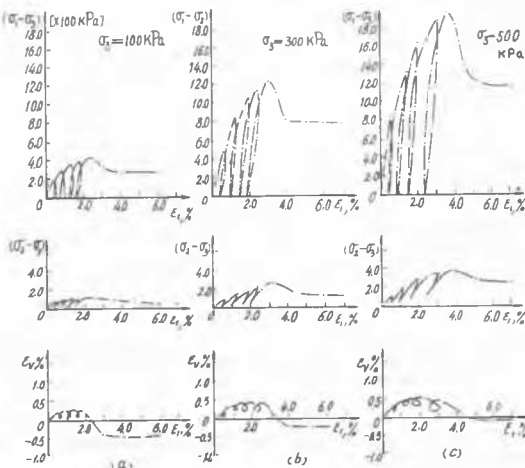


Fig.4 Plane strain test curves for sand under repeatedly loading-unloading condition

THREE DIMENSIONAL (3-D) YIELD FUNCTION IN PRINCIPAL STRESS SPACE

Most of the boundary-value problems in earthwork and foundation engineering belong to plane strain or 3-D states. Experimental results indicate that yield function derived from conventional triaxial tests is not applicable to these cases. It is, therefore, necessary to seek the form of yield surface and expression of stress-strain relation for plane strain condition and in 3-D principal stress space  $(p, q, \theta)$ , and examine the possibility of determining the relevant parameters for these cases by using directly the result of simple conventional triaxial tests.

3-D Principal Stress Space

Following symbols are used in this paper:

- $I_1$  : first stress invariant
- $J_2, J_3$  : second and third deviatoric stress invariants
- $J_2', J_3'$  : second and third invariants of plastic deviatoric strain increment
- $p$  : octahedral normal stress
- $q$  : octahedral shear stress

$\epsilon_V^P$  : octahedral plastic normal strain  
 $\bar{\epsilon}^P$  : octahedral plastic shear strain  
 $\theta, \psi$  : Lode angle for stress and plastic strain increment  
 $H$  : Work hardening parameter

$$H = \frac{1}{1+k} \left( \frac{m_6 + \epsilon_V^P - m_3 \bar{\epsilon}^P}{m_4} \right)^{m_5} \quad (4)$$

in which  $A, B, m_3, m_4, m_5, m_6$  are experimental constants determined from data of isotropic consolidation and conventional triaxial tests. The associated flow rule may then be expressed as

$$d\epsilon_V^P = d\lambda \frac{\partial f}{\partial p}$$

$$d\bar{\epsilon}^P = d\lambda \frac{\partial f}{\partial q}$$

$$\psi = \theta$$

Such a flow rule is not applicable, however, to 3-D yield functions containing third stress invariant such as shown in Eq (1). In this case, the following flow rule should be used instead (Li, 1984):

$$d\epsilon_V^P = d\lambda \frac{\partial f}{\partial p} \quad (5)$$

$$d\bar{\epsilon}^P = d\lambda \left( \left( \frac{\partial f}{\partial q} \right)^2 + \left( \frac{1}{q} \frac{\partial f}{\partial \theta} \right)^2 \right)^{\frac{1}{2}} \quad (6)$$

$$\psi = \frac{1}{3} \sin^{-1} \left( \frac{-\sqrt{3}}{18J_2} (27J_2 J_3 \sqrt{J_2} \left( \frac{\partial f}{\partial q} \right)^3 - 9J_2 \cdot \sqrt{4J_2^3 - 27J_3^2} \cdot \left( \frac{\partial f}{\partial q} \right)^2 \cdot \frac{\partial f}{\partial \theta} - 27J_3 \sqrt{J_2} \frac{\partial f}{\partial q} \left( \frac{\partial f}{\partial \theta} \right)^2 + \sqrt{4J_2^3 - 27J_3^2} \left( \frac{\partial f}{\partial \theta} \right)^3) / \left( \left( \frac{\partial f}{\partial q} \right)^2 + \left( \frac{\partial f}{\partial \theta} \right)^2 \frac{1}{3J_2} \right)^{\frac{3}{2}} \right) \quad (7)$$

Eqs (6) and (7) indicate that the direction of plastic strain increment vectors on  $\pi$ -plane no longer coincides with the direction of octahedral shear stresses and they are not in proportion to each other any more.

Yield Function in 3-D Stress Space

(1) Determination of yield loci on  $\pi$ -plane by use of test data.

True triaxial tests with  $\theta = \pm 30^\circ, \pm 16.1^\circ, 0^\circ$  (corresponding to  $b=0, 0.25, 0.50, 0.75, 1.00$ ) have been performed on medium dense Chengde sand. Fig.7 illustrates the direction of plastic strain increment vectors obtained. It is readily seen

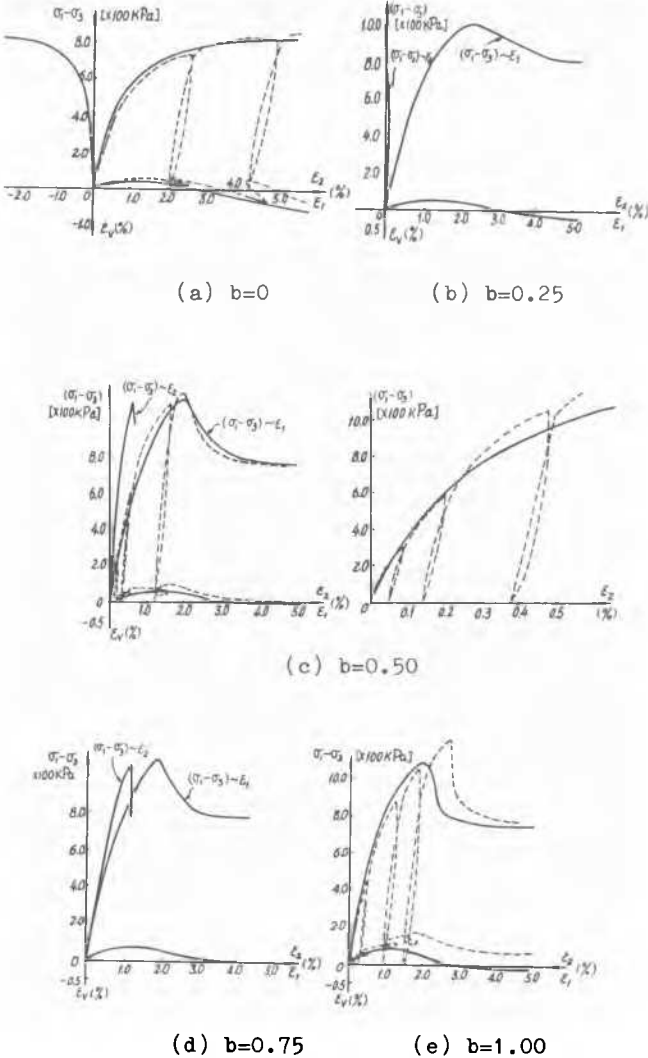


Fig.6 Typical true triaxial test curves ( $\sigma_3 = 300$  kpa) for sand

For isotropic material, the generalized yield function is

$$f(I_1, J_2, J_3, H) = 0 \quad (1)$$

or  $f(p, q, \theta, H) = 0 \quad (2)$

If yield surfaces are axisymmetric about the space diagonal, then the yield function may be reduced to the form of

$$f = f(p, q, H) = 0 \quad (2')$$

It has been proved that on basis of conventional triaxial test results the yield function and strain hardening parameter for this case may be written as

$$f = \left( \frac{p-H}{Ah} \right)^2 + \left( \frac{q}{Bh} \right)^2 - 1 = 0 \quad (3)$$

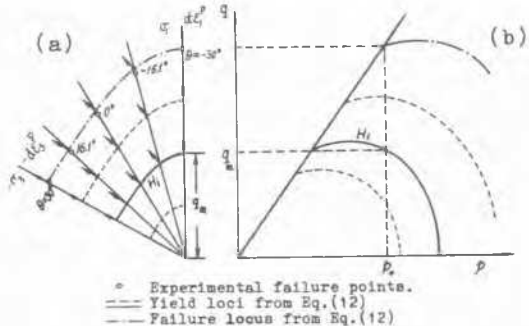


Fig.7 Yield loci on (a)  $\pi$ -plane with  $p=p_0$ ; (b)  $p$ - $q$  plane with  $\theta = -30^\circ$

that, when associated flow rule is adopted, the yield loci on  $\pi$ -plane are a family of similar curves which may be represented as

$$q = q_m \cdot \alpha(\theta) \quad (8)$$

in which  $q_m$  is the octahedral shear stress under conventional triaxial compression;  $\alpha(\theta)$  is the shape function which may be determined from test data either by curve fitting method or the method to be described later.

(2) Form of yield function in 3-D stress space. As stated above, the yield function obtained from conventional triaxial compression tests may be written as

$$f = \left(\frac{p-H}{AH}\right)^2 + \left(\frac{q_m}{BH}\right)^2 - 1 = 0 \quad (3)$$

Yield loci of  $H=H_i$  surface on  $\pi$ -plane and  $p$ - $q$  plane are shown in Figs. 7(a) and 7(b).  
On  $p$ - $q$  plane with  $\theta=-30^\circ$ ,

$$q_m = BH_i \sqrt{1 - \left(\frac{p_0 - H_i}{AH_i}\right)^2} \quad (9)$$

On  $\pi$ -plane with  $p=p_0$ ,

$$q = q_m \cdot \alpha(\theta) = BH_i \sqrt{1 - \left(\frac{p_0 - H_i}{AH_i}\right)^2} \cdot \alpha(\theta) \quad (10)$$

Taking  $p_0$  and  $H_0$  as variables  $p$  and  $H$ , the yield surface in 3-D stress space may be obtained from Eqs (9) and (10) as follows:

$$f = \left(\frac{p-H}{AH}\right)^2 + \left(\frac{q}{BH \cdot \alpha(\theta)}\right)^2 - 1 = 0 \quad (11)$$

(3) Determination of shape function  $\alpha(\theta)$  from conventional triaxial compression test. It has been proved (Li, 1984) that in elasto-plastic model with yield surface and workhardening parameter as represented by Eqs (3) and (4), the failure locus and yield locus on  $\pi$ -plane are similar. This may also be seen from the test result shown in Fig.7. It is thus possible to determine the shape function  $\alpha(\theta)$  from failure locus in accordance with the following requirements:

- i) It must satisfy the boundary condition of  $\alpha=1.0$ ,  $\partial\alpha/\partial\theta=0$ , when  $\theta=-30^\circ$   
 $\alpha=k$ ,  $\partial\alpha/\partial\theta=0$ , when  $\theta=30^\circ$   
in which  $k$  is the ratio of strength obtained in triaxial extension test to that obtained in triaxial compression test.  $k$  may either be determined from test data or by use of Mohr-Coulomb or Lade-Duncan failure criterion. For instance, in case of cohesionless soil,  $k$  may be determined from Mohr-Coulomb failure criterion in terms of internal friction angle  $\phi$  of the soil, i.e.  $k=3-\sin\phi/3+\sin\phi$ .
- ii) According to Drucker's postulate,  $\alpha(\theta)$  must be a convex curve. In the extreme case of  $\phi=0^\circ$  ( $k=1.0$ ), the simplest convex curve is a circle, i.e.  $\alpha(\theta)=1.0$ . In another extreme case of  $\phi=90^\circ$  ( $k=1/2$ ), the only non-concave curve is a straight line.

Therefore, two circular segments, with different radii and centers, that satisfy all above requirements may be used to represent the yield loci. They are smoothly connected to each other

at  $\theta=\theta_0=\arctan \frac{1}{3} \frac{(4k^3-4k^2+k-3)}{(4k^3+3k+1)}$ . By curve fitting

method, the shape function  $\alpha(\theta)$  may then be expressed as follows:

$$\theta > \theta_0 \quad \alpha_1(\theta) = \frac{1}{k(2k-1)} \left( \frac{\sqrt{(1-k)^2(1+2k^2)^2 \cos^2(30^\circ-\theta) + k^2(2k-1)(2+3k^2-2k^3-2k)-(1-k)(1+2k^2)} \cos^2(30^\circ-\theta)}{k^2(2k-1)(2+3k^2-2k^3-2k)-(1-k)(1+2k^2)} \right) \quad (12a)$$

$$\theta < \theta_0 \quad \alpha_2(\theta) = \frac{1}{(1+2k-2k^2)} \left( \frac{\sqrt{(1-k)^2(2k^2+k+2) \cos^2(30^\circ+\theta) + (1-k)^2(2k^2+k+2)^2 \cos^2(30^\circ+\theta)}}{(1+2k-2k^2)(4k^3-4k^2+4k-3)} \right) \quad (12b)$$

As can be seen from the equations, shape function  $\alpha(\theta)$  is readily determined once  $k$  is evaluated from conventional triaxial tests.

Comparison of Calculated and Measured Stress-Strain Relationships for Medium Dense Chengde Sand under Plane Strain Condition

The elasto-plastic modulus matrix for the plane

strain case may be derived by making use of the three basic conditions:  $d\epsilon_2=0$ ,  $d\gamma_{yz}=0$ ,  $d\gamma_{xz}=0$ .

Then, by substituting the parameters determined from conventional triaxial compression tests into this matrix, we can predict the stress-strain relation for the medium dense Chengde sand under plane strain condition. Fig.8 shows the calculated stress-strain relation in comparison with the results of plane strain tests performed (Li Shu-Qin, 1982). Satisfactory agreement is seen.

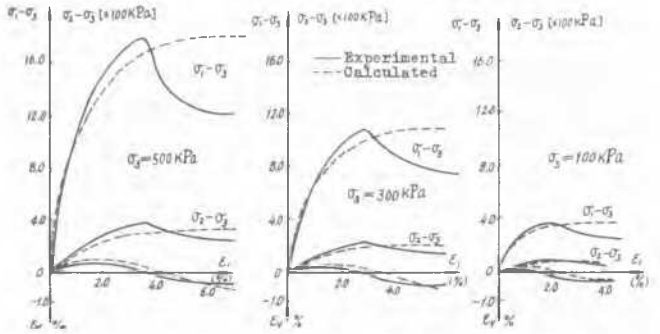


Fig.8 Experimental and calculated stress-strain curves for Chengde sand under plane strain condition

CONCLUSION

- (1) Experiments made under complex stress states reveal that on  $\pi$ -plane the direction of octahedral plastic shear strain increment vectors does not coincide with that of deviatoric stresses. Therefore, it is not appropriate to use the yield function derived from conventional axisymmetric triaxial compression tests to solve the geotechnical boundary-value problems belonging to plane strain or 3-D stress states.
- (2) It has been proved theoretically that in 3-D principal stress space, octahedral plastic strain increments are functions not only of  $\partial f/\partial p$  and  $\partial f/\partial q$  but also of  $\partial f/\partial \theta$ , and the plastic strain increment Lode angle  $\psi$  is not equal to the stress Lode angle  $\theta$ .
- (3) The yield function in 3-D principal stress state has been derived and it is verified by comparing the plane strain test results with that calculated by this model.

The writers are grateful to Prof. Huang Wen-Xi under whose guidance this study has been carried out

REFERENCES

Huang, Wen-Xi (1980). Effect of work hardening rules on the elasto-plastic matrix. Soils under Cyclic and Transient Loading, pp.227-283 A.A. Balkema, Rotterdam.  
Huang, Wen-Xi; Pu, Jia-Liu and Chen, Yu-Jiong (1981). Hardening rule and yield function for soils. Proc. 10th Int. Conf. Soil Mech. Found. Engg, (1), 631-634, Stockholm.  
Li, Shu-Qin (1982). Experimental study on constitutive relation for cohesionless soils in plane strain condition. MS<sub>C</sub> Thesis (in Chinese), Tsinghua University.  
Li, Guang-Xin (1984). Three dimensional yield function and its verification. PhD Thesis (in Chinese), Tsinghua University.